1H NMR depth profiles combined with portable and micro-analytical techniques for evaluating cleaning methods and identifying original, non-original, and degraded materials of a 16th century Italian wall painting

^{1}H NMR DEPTH PROFILES COMBINED WITH PORTABLE AND MICRO-ANALYTICAL TECHNIQUES FOR EVALUATING CLEANING MENTHODS AND IDENTIFYING ORIGINAL, NON-ORIGINAL, AND DEGRADED MATERIALS OF A 16TH CENTURY ITALIAN WALL PAINTINGS

Di Tullio Valeria; Sciutto Giorgia; Proietti Noemi; Prati Silvia; Mazzeo Rocco; Colombo Chiara; Cantisani Emma; Romè Velentina; Rigaglia Davide; Capitani Donatella.

Cite this article as:

Di Tullio, V., Sciutto, G., Proietti, N., Prati, S., Mazzeo, R., Colombo, C., Cantisani, E., Romè, V., Rigaglia, D., Capitani, D., Microchem J (2018) 141:40

DOI: https://doi.org/10.1016/j.microc.2018.04.034

First Online: 01 May 2018
Available at:
https://reader.elsevier.com/reader/sd/pii/S0026265X17308639?token=AA306417AF0F463232FFCF7999687B41A5C8AEA65359D3795CBECAA95DED6418ED0981F0AEF098C113912E40A517EBBC

Microchemical Journal xxx (xxxx) xx-xx

Contents lists available at ScienceDirect

Microchemical Journal

journal homepage: www.elsevier.com/locate/microc

^{1}H NMR depth profiles combined with portable and micro-analytical techniques for evaluating cleaning methods and identifying original, non-original, and degraded materials of a 16th century Italian wall painting

Valeria Di Tullio[a,b,*], Giorgia Sciutto[c], Noemi Proietti[a], Silvia Prati[c], Rocco Mazzeo[c], Chiara Colombo[d], Emma Cantisani[d], Valentina Romè[e], Davide Rigaglia[e], Donatella Capitani[a]

[a] Magnetic Resonance Laboratory "Annalaura Segre", Institute of Chemical Methodologies (IMC), CNR, Via Salaria km. 29,300, 00015 Monterotondo (RM), Italy
[b] Metropolitan Museum of Art, 1000 5th Ave, New York 10028, NY, USA
[c] University of Bologna, Department of Chemistry "G. Ciamician" Via Guaccimanni 42, 48121 Ravenna, Italy
[d] Institute for the Conservation and Valorization of Cultural Heritage (ICVBC), CNR, Via Madonna del Piano, 10, 50019, Sesto Fiorentino (FI), Italy
[e] Restorer, Impresa individuale, Italy

ARTICLE INFO

Keywords:
Unilateral NMR
Infrared spectroscopy
Wall painting
Cleaning treatments
Carboxylates

ABSTRACT

In this study, portable NMR was applied to monitor and evaluate cleaning treatments on the surface of a 16th century Italian wall painting.

Due to the complexity of the state of degradation of the wall painting, a campaign of measurements was carried in situ to evaluate the performance of traditional and innovative eco-friendly cleaning systems such as sulphate-reducing bacteria *D. vulgaris* confined in hydrogels, and to compare two different cleaning systems used to remove a degraded hydrophobic organic layer.

Specifically, NMR stratigraphy allowed to determine the thickness of the organic layer covering the surface of the wall painting, its distribution in the wall painting, the presence of residues after applying the cleaning treatment, and to evaluate and compare the effectiveness of applied treatments. A new analytical parameter here named *the solubilization degree of the cleaning system* permitted the selection of the most performing treatment. ^{1}H NMR depth profiles allowed to evaluate changes in the permeability of the wall painting caused by the presence of organic substances during the application of water-based cleaning systems, and to evaluate the water content and its depth of penetration in the wall painting. Changes in permeability were estimated calculating another new analytical parameter, i.e. *the percentage of water saturation* before and after the application of the cleaning treatment. Depth profiles also permitted the evaluation of the degree of wettability of the wall painting surface as a function of the time of application, and the obtainment of a detailed information about the interaction between water molecules, the gel network and the surface of the wall painting. Finally, to obtain the chemical characterization of the artefact surface a multi analytical approach was applied using both portable and micro-invasive analytical methodologies.

1. Introduction

Among restoration procedures, the cleaning of artefacts is one of the most delicate and potentially damaging operation. It is well known that a cleaning treatment is aimed at removing different type of undesired layers of degradation (i.e. crusts, salts efflorescence, metal stains) and it has to respect diverse requirements. High performing cleaning systems should have high physico-chemical stability, weak aggressiveness to the material. In addition, cleaning systems should be environmental friendly, and not toxic to the operator, and should be able to control the evaporation and penetration of solvents into the porous structure without leaving residual materials on the surface of the artefact. Furthermore, if the artefact experienced a number of retouching, a cleaning system should provide high selectivity between the materials to be removed and those to be preserved [1–3]. The monitoring of cleaning treatments, the characterization of the constitutive materials and the knowledge of interactions among these materials and cleaning treatments are a fundamental step in a restoration project as well as in research projects focused on the development of new cleaning systems.

Efficacy, suitability of products and procedures should be subjected

* Corresponding author at: Magnetic Resonance Laboratory "Annalaura Segre", Institute of Chemical Methodologies (IMC), CNR, Via Salaria km. 29,300, 00015 Monterotondo (RM), Italy.
E-mail address: valeria.ditullio@cnr.it (V. Di Tullio).

https://doi.org/10.1016/j.microc.2018.04.034
Received 30 August 2017; Received in revised form 2 April 2018; Accepted 30 April 2018
Available online 01 May 2018
0026-265X/

to a preliminary evaluation on selected area of the surface artefact or on specimens prepared in laboratory. The aim of cleaning trial area should be to determine the suitably of the cleaning method for the object and the degree of cleaning that can be achieved. Nevertheless, the simultaneous presence of ancient, non-original, and degraded materials makes both the analytical characterization and the study of interactions very challenging. Due to the difficulty to collect samples from precious artefacts and the complexity of simulating a surface of an ancient naturally degraded artefact, the use of portable instrumentation is highly advisable to monitor and evaluate cleaning treatments directly on the surface of the artefact.

Several analytical methodologies, such as GC/MS, Raman and FT-IR spectroscopy, have been applied to evaluate the performance of cleaning products and to chemically characterize the presence of organic residual materials on the surface of artefacts such as paintings, papers and lapideous materials [4–8]. Although these analytical methodologies are very powerful techniques to obtain a chemical characterization of materials, they have been rarely applied to monitor and to evaluate the thickness reduction and the degree of removal of layers subjected to a cleaning treatment.

Furthermore, the depth of penetration of solvents used in cleaning treatments and the distribution of residues inside the artefact are important parameters to be evaluated during a cleaning treatment. The capability of solvents to diffuse through a porous material affects the performance of a cleaning system that has to guarantee a high selectivity and provide a superficial action of solubilization. To remove undesired materials distributed in a porous network and obtain a swelling action on thick materials that are difficult to solubilize, some degree of penetration of solvent can be desirable. On the contrary, a high degree of penetration of solvents can cause a dispersion of residual materials in deeper layers of the artefact triggering off, over time, serious and often irreversible processes of alteration. Evaluating the depth of penetration of solvents during a cleaning treatment can help at modulating the solubilization degree of the cleaning system and at controlling an excessive or inadequate penetration within the artefact.

Portable nuclear magnetic resonance (NMR) allows measurements to be performed in situ without any sampling. The magnetic field is applied to one side of the object, thus the integrity and the dimension of the object under investigation are fully preserved [9,10]. Although the magnetic field of this sensor is inhomogeneous, it is possible to measure NMR parameters such as proton density, relaxation times, self-diffusion coefficients, and even to collect correlation maps [11]. Due to the capability to measure the hydrogen content as a function of depth of measurement, unilateral NMR is a very powerful tool to scan layers constituted by organic substances as well as to measure the water content absorbed by porous materials [11–13]. In recent years, unilateral NMR has been previously used to evaluate restoration treatments applied on porous stones and painted surfaces [14–19], to explore the interaction between lead white and collagen-based binders in a medieval-illuminated manuscript [20], and to study new and artificially aged vegetable leathers [21].

In this study, portable NMR was used to investigate the possibility of establishing an analytical protocol to evaluate the action of cleaning products based on micro-emulsion and solvent gels, and to detect the possible presence of residual materials on the surface of the artefact. Because the reduction of thickness of layers under removal is strictly correlated with the power of cleaning system, hydrogen depth profiles were collected by unilateral NMR on the surface of the painting before and after the cleaning treatment to evaluate the solubilization degree of the cleaning system applied.

Unilateral NMR was applied to compare and monitor the penetration depth, and the mobility and diffusivity of water in two types of hydrogel/bacteria systems applied on the surface of a degraded wall painting. Since the penetration of a solvent also depends on the duration of the application of the treatment itself, different regions of the wall painting treated for varying lengths of time were investigated. In fact, the possibility of optimizing the length of time of the treatment application would also be of help during restoration and maintenance.

Finally, to obtain the chemical characterization of the artefact surface before and after the cleaning treatment a multi analytical approach was applied using both portable and micro-invasive analytical methodologies.

2. Materials and methods

The cleaning procedure was planned with the dual purpose of removing both the degraded non-original translucent layer and the very thick salt efflorescences.

A micro-emulsion and a solvent gel were used to remove the non-original translucent substance, and their efficiency was compared. Poultices of sulphate-reducing bacteria entrapped in two different type of hydrogels were applied to remove salt efflorescences affecting the wall painting surface.

In order to investigate the performance of these cleaning treatments as well as to obtain chemical characterizations of the surface before and after the cleaning, a multi-analytical study was carried out in two successive steps. During the first step, a full characterization of the materials of the wall painting was carried out by portable infrared spectroscopy (FTIR), and a set of micro-invasive techniques such as ^{13}C Cross Polarization Magic Angle Spinning NMR spectroscopy (^{13}C CPMAS NMR), scanning electron microscopy-energy dispersive spectroscopy (SEM-EDS), μFTIR in attenuated total reflection (ATR), and X-ray diffraction (XRD), was applied. To investigate the distribution of elemental and molecular components of original and non-original materials, ATR-FTIR and EDS mappings on cross-sections were carried out.

During the second step areas M1-M4 on the surface of the wall painting surface were selected to monitor the effect of cleaning treatments by unilateral NMR and portable FTIR, see Fig. 1. Eight samples, S1-S8 were collected from the wall paintings to perform analyses in laboratory.

2.1. The wall painting

The pictorial cycle garnishing the Vitelleschi's chapel of the Tarquinia cathedral was painted by Antonio da Viterbo nicknamed *Il Pastura* (1450–1516) who was most likely a Perugino's scholar [22] and worked with Pinturicchio to decorate the Borgia Apartment in Vatican City, Rome, Italy. The chapel decoration represents the *Prophets and Sybils* and *Coronation of the Virgin* on the vault, the *Marriage of the Virgin* on the right side of the chapel, *Birth of the Virgin Mary*, *the /Pietà, the Meeting of Joachim and Anna* and *the Virgin and Child* on the left side. In 1642 a fire destroyed the bottom of the chapel and damaged the painted surface of the vault. Restoration works were carried out in 1877, 1939, 1979, and 2013. The latest restoration was aimed at the renovation of the roof in order to avoid rainwater infiltration that had previously affected the wall painting causing salt efflorescences on the painted surface. Repeated crystallization cycles had caused loss of cohesion and detachment of the pictorial layers from the plaster and compromised the appearance and the chromatics of the painting. A thick translucent layer and darkened areas were also observable on the painted surface along with several pictorial reintegrations due to previous restorations.

2.2. Cleaning products and application

An oil-in-water micro-emulsion containing an anionic surfactant was used to remove the translucent layer from the wall painting [23,24]. The oil-in-water micro-emulsion (Nanorestore Cleaning Apolar Coating, CSGI Firenze, Italy) entraps 1-pentanol, an anionic surfactant, namely sodium-dodecyl-sulphate, and p-xylene. The micro-emulsion was daubed on paper pulp and applied on the surface of the wall painting for 1 h and then it was washed by water.

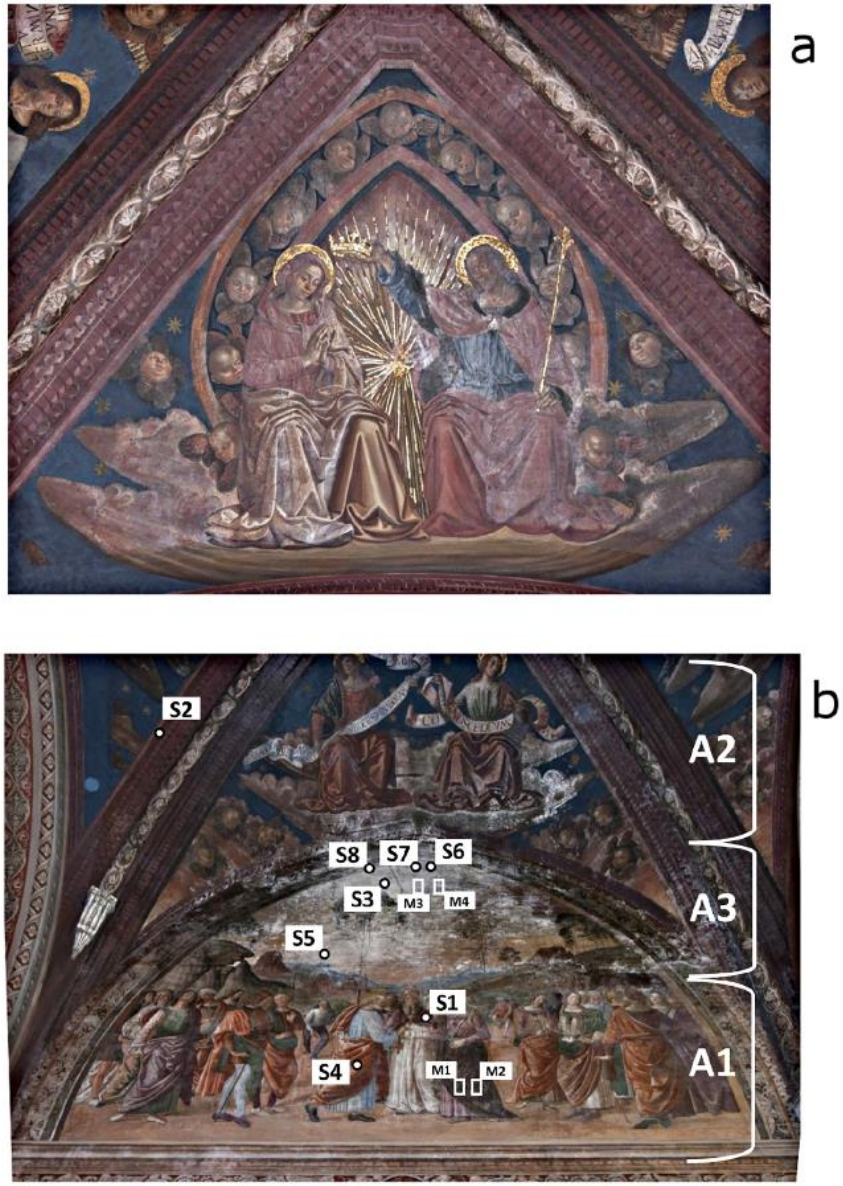

Fig. 1. a) Coronation of the Virgin, vault. b) Marriage of the Virgin, right wall. Labels M1, M2, M3 and M4 indicate the selected areas treated with solvent gel, microemulsion, Carbogel/bacteria, and Vanzan/bacteria, respectively. Labels S indicate the sampled regions.

The solvent gel was prepared by ligroin, isopropyl alcohol and methyl ethyl ketone (55:19:26 volume). The mixture was gelified in a solution of poly-acrylic acid and ethomeen C-12. The solvent gel was daubed on Japanese paper, applied on the surface of the wall painting, and covered with a film of PVC for 1 h. The solvent gel was finally removed with the same solution used for the preparation.

To remove salts efflorescences affecting the region under the vault of the chapel, sulphate-reducing bacteria entrapped in hydrogels were prepared. The use of *Desulfovibrio vulgaris* bacteria confined in hydrogels has become a quoted method to remove sulphates from stone material belonging to cultural heritage. Thanks to their metabolism, sulphate-reducing bacteria *D. vulgaris* are able to reduce SO_4^{2+} ions to H_2S [25,26]. The viscosity of the gel reduces the diffusion of the liquid phase in the porous structure and increases the selectivity of the cleaning action. A 2% Carbogel (CTS srl, Vicenza, Italy) and a 3% Vanzan NFC (CTS srl, Vicenza, Italy) gels were prepared by swelling the powder in water. Carbogel is a polymer of acrylic acid cross-linked with alkenyl ethers of sugars or poly alcohols. Vanzan is a xanthan gum with high molecular weight exocellular polysaccharide derived from the bacterium *Xanthomonas campestris* using a natural, aerobic fermentation process. The cleaning formulations were prepared by dissolving 2.5 g lyophilized bacteria in 2 l water, 50 ml of this suspension was added to 100 ml gel. Gels with bacteria were applied on the surface of the wall painting for 2 and 4 h.

2.3. Unilateral NMR and solid state NMR spectroscopy

Depth profiles, relaxation times, and self-diffusion coefficients were measured at 0.36 T (13.62 MHz) with a unilateral NMR instrument constituted by an electronic unit from Bruker Biospin interfaced with a purposely built single-sided sensor ACT by RWTH Aachen University, Aachen, Germany [12]. This sensor generates a magnetic field with an extremely uniform gradient to resolve the near surface structure of arbitrary large objects. Measurements can be performed at different depth of measurements (1,3, 5 and 10 mm) changing three spacers in the probe. Due to the geometry of the probe, each spacer requires a

different duration of π/2 pulse, a duration of echo time, a nominal resolution and a signal acquisition window. The selection of the proper depth of measurement and experimental conditions depends on the type of material to be analyzed and on the condition of the artefact surface. In the case of application of the solvent gels/microemulsion a spacer was inserted in the probe to scan the artefact from the outermost surface to a depth of 3 mm. In the case of application of hydrogel/bacteria cleaning systems, in order to scan the water distribution through the artefact, a deeper deep of measurement had to be achieved, as a consequence the 5 mm spacer was inserted in the probe. ^{1}H NMR depth profiles were collected on the translucent layer of the wall painting before and after applying cleaning treatments. Because the translucent layer showed a very short transverse magnetization decay, ^{1}H depth profiles were obtained averaging the amplitude of the first two echoes obtained by a CPMG pulse sequence acquired with a time domain of 32 echoes, an echo time of 44.2 μs, and a nominal resolution of 70 μm. The single sided sensor was repositioned in steps of 100 μm to scan the wall painting up to a depth of 3 mm.

^{1}H NMR depth profiles were also collected before and after the application of hydrogel/bacteria cleaning systems to evaluate the water content absorbed by the wall painting. Profiles were obtained as the addition of the amplitude of the first four echoes obtained by a CPMG pulse sequence acquired with a time domain of 32 echoes, with an echo time of 55 μs and a nominal resolution of 55 μm. The single-sided sensor was repositioned in steps of 250 μm to scan the wall painting up to a depth of 3.6 mm.

To obtain the total hydrogen content, integrals of profiles were calculated by numerical integration applying the Newton-Cotes quadrature rule.

Longitudinal relaxation times T_1 were measured with a Saturation Recovery pulse sequence followed by a CPMG-train in the detection period to increase the sensitivity [12]. Effective transverse relaxation times T_{2eff} [27,28] were measured with a CPMG pulse sequence, 4096 echoes were recorded on the gel with an echo time (2τ) of 71.2 μs. The inhomogeneous magnetic field of unilateral NMR is a further source of relaxation which shortens the measured T_{2eff} values of the gel, making them definitively shorter than those which would be measured in a homogeneous field. Data processing was performed fitting the longitudinal magnetization decays to the following equation: $M_z(\tau) = M_0\left(1 - e^{\frac{-2\tau}{T_1}}\right)$.

Transverse magnetization decays were fit using both a bi-exponential decay function and an Inverse Laplace Transformation (ILT). Both methods provided robust and consistent values. In the paper the T_2 distributions obtained by ILT, were reported. This representation is very suitable in the case of heterogeneous systems which usually exhibit multiple relaxation times. In this representation peaks of the distribution are centred at the most probable T_2 values while peak areas correspond to the weight of T_2 components.

Before fitting, the sum of weights was normalized to 100%.

The uncertainty associated with T_1 and T_{2eff}, was obtained by repeating the measurement three times on each sample.

Self-diffusion coefficients D were measured with a steady gradient (SG) of 14.28 T/m using a stimulated echo (SGSTE) pulse sequence followed by a CPMG echo train to improve the SNR (signal to noise ratio). In SGSTE, the attenuation of the spin echo signal resulting from the dephasing of nuclear spins is used to measure molecular displacement, the STE sequence was characterized by two encoding periods (τ_1), separated by a well-defined evolution time (Δ) during which the diffusion takes place. The amplitude of a stimulated echo relaxes with T_1 during Δ, when the magnetization is stored as longitudinal magnetization. The normalized attenuation is given by the following equation:

$$\ln\left(\frac{A}{A_0}\right) = -\gamma^2 G^2 \tau_1^2 \left(\Delta + \frac{2}{3}\tau_1\right) D - \frac{2\tau_1}{T_2} - \frac{\Delta}{T_1}$$

where A_0 is the amplitude of the echo at a very short time τ_1, D is the self-diffusion coefficient, Δ is the diffusion time, G (14.28 T/m) is the magnetic field gradient, γ is the ^{1}H gyromagnetic ratio ($2.6752 \times 10^{8}\ s^{-1}\ rad\ T^{-1}$), and T_1 and T_2 are the longitudinal and transverse relaxation times, respectively. For large D values, strong magnetic field gradient, and provided that $\tau_1 << T_2$, and $\Delta << T_1$, diffusion terms dominate over relaxation terms and the self-diffusion coefficient may be obtained by the following equation:

$$\ln\left(\frac{A}{A_0}\right) = -\gamma^2 G^2 \tau_1^2 \left(\Delta + \frac{2}{3}\tau_1\right) D$$

The uncertainty associated with D was obtained by repeating the measurement three times on each sample. Both T_1, T_2 and the self-diffusion coefficient of water, were measured in the first millimeter of gels before the application of the cleaning system on the wall painting.

Solid-state ^{13}C CPMAS NMR spectra were performed at 100.13 MHz on a Bruker Avance 400 spectrometer. Samples were packed into 4 mm zirconia rotors with an internal volume reduced to 25 μl, and sealed with Kel-F caps. The spin-rate was kept at 7000 Hz. The 90° pulse width was 4 μs, the relaxation delay was 3 s, and the contact time for the cross-polarization was 1.5 ms. The cross-polarization was performed applying the variable spin-lock sequence RAMP–CPMAS, and the RAMP was applied on the ^{1}H channel. The center of the RAMP was set to the first matching sideband taking advantage of the faster cross-polarization rate compared to that of the matching center band. Spectra were obtained using 1024 data points in the time domain, zero-filled, and Fourier transformed.

2.4. Reflection infrared spectroscopy and infrared microscopy

Infrared spectra were recorded using a compact portable FTIR spectrometer (ALPHA, Bruker Optics, Germany/USA-MA) equipped with a SiC globar source, a "rock solid"-design interferometer (with gold mirrors) and a DLaTGS detector. Measurements were performed by an external reflectance module with an optical layout of 22°/22°. Pseudo-absorption spectra [log(1/R); R = reflectance] were acquired from areas with a diameter of about 5 mm in the spectral range of 7000–375 cm^{-1}, with a resolution of 4 cm^{-1} and using 186 scans. Spectra from a gold flat mirror were used as background.

To better clarify the molecular constituents and the distribution of the different components along the non-original and original painting layer and plaster of the wall painting, an ATR-FTIR mapping on cross-sections of three samples was carried out. Sample S1 was obtained from a region covered by a translucent layer in the bottom of the wall painting (region A1). Sample S2 was obtained from a region of the upper frame of the ceiling vault (region A2), while sample S3 was obtained from a region just under the vault where abundant salts efflorescence were observed (region A3), see Fig. 1. A thermos Nicolet (Thermo Fisher Scientific) iN10 M X imaging microscope fitted with a mercury-cadmium-telluride (MCT) detector cooled by liquid nitrogen, was used. Mid infrared spectra (4000–675 cm^{-1}) were recorded in attenuated total reflection (ATR) mode by means of a germanium crystal (refractive index = 4) operating in contact with the surface of the samples. The spectra were obtained by averaging 64 acquisitions and with 4 cm^{-1} spectral resolution. A dedicated software OMNIC Picta (Thermo Fisher Scientific) was used to process the spectra. Sample stratigraphies submitted to the analysis were prepared applying the double embedding procedure [29]. In more detail, the micro fragment was preliminary embedded in KBr pellets. Afterwards, the pellet obtained was reduced in the external part and submitted to the polyester-resin embedding procedure. A dry polishing procedure was applied using Micro-Mesh® silicon carbide papers (Micro-Surface Finishing Inc., Wilton, USA) with successive grid from 2400 up to 12,000.

2.5. OM, SEM-EDS and XRD

Cross-sections were embedded in an epoxy resin and thereafter polished using diamond pastes (6 µm and 2 µm). Morphological and stratigraphic investigations were carried out by optical microscopy (OM) and scanning electron microscopy (SEM) coupled with energy dispersive X-ray spectroscopy (EDS). OM images were collected with a Leitz Ortholux microscope equipped with a Nikon DS-5M/USB digital camera. SEM investigation by back-scattered electrons (BSE) and EDS analysis were carried out on cross sections with (SEM) JEOL 5910 LV equipped with an IXRF-2000 X-ray spectrometer operating in energy dispersion. Sections were mounted onto SEM stubs and analyzed in low vacuum mode, the composition was investigated by EDS spectra recorded between 0 and 20 keV acceleration voltage.

XRD analysis was performed by a PANalytical X'Pert Pro X-ray diffractomer. X-ray powder diffraction patterns were collected in the $3^\circ < 2\theta < 70^\circ$ range according to the step scanning procedure with Cu K_α radiation = 1.5405 Å. The tube operated at 40 KV and 30 mA. Data were processed using the Highscore software, a zeroground support was applied before data processing.

3. Results and discussion

3.1. Characterization of constitutive materials of the wall painting by micro-analytical techniques

The cross section S1 was characterized by the presence of a thick red layer (layer 1, Fig. 2a) composed mainly by silicates (band at 1080 cm^{-1}, Si-O stretching), ascribable to the use of an earth-based pigment, and calcium carbonate (band at 875 cm^{-1}, $CaCO_3$ bending) belonging to the original pictorial layer and plaster. It was possible to observe as the uppermost layer a fluorescent material probably applied as varnish (layer 2, Fig. 2b). Molecular mapping analysis allowed to identify and clearly locate beeswax, thanks to the presence of the diagnostic band at 730 cm^{-1} (CH rocking vibration mode). Calcium carboxylates were also detected at the interface with the ground layer due to the diagnostic double bands at 1576 and 1538 cm^{-1} probably produced by the interaction between the fatty organic binder and the calcium salt. Calcium oxalates (band at 1320 cm^{-1} associated to the COO− symmetric stretching mode) were identified overall the investigated area. On the other hand, no peculiar absorption bands referred to the presence of an organic binder were observed. Even if this outcome may suggest the use of a *secco* technique, the relative small amount of binder usually applied in a painting might be hidden in mid-IR spectra by the intense absorption band of the inorganic components.

The cross–section of sample S2 showed a reddish layer with black crystals over the ground layer, see Fig. 3a. The mapping allowed to locate silicates and quartz as principal components. In addition, gypsum was also detected thanks to the band at 3530 cm^{-1} (OH stretching), together with calcium carbonate and traces of organic substances, as indicated by the CH stretching absorption bands at 2850 and 2918 cm^{-1}. The pigment layer 2 probably conferred the gray-blue tonality of the area where the sample was collected. Gypsum (band at 3530 cm^{-1}), was identified as main component possibly originating by an alteration process. Interestingly, its presence was detected overall the paint stratigraphy not only in the uppermost layer where the highest concentration was found. Moreover, also silicates and traces of organic material were present. The thin layer 3, most likely applied as finishing layer, was characterized by a bluish fluorescence emission colour, Fig. 3b. Analytical investigation allowed to identify a fatty substance due to presence of the carbonyl absorption band at 1735 cm^{-1}. Both these experimental evidences allowed to hypothesize the presence of beeswax. The interaction between the organic coating and calcium carbonate possibly led to the formation of calcium carboxylates as degradation product.

Molecular mapping on the cross-section of sample S3 was aimed at characterizing the efflorescences on the painted surface, see Fig. 4. Gypsum was clearly located in the uppermost layer (layer 3) and in the neighboring layer 2 together with traces of organic substances (band at 2918 cm^{-1}), whose precise chemical nature was uncertain due to the limited amount present. In layer 1 it was possible to localize silicates mixed with calcium carbonate.

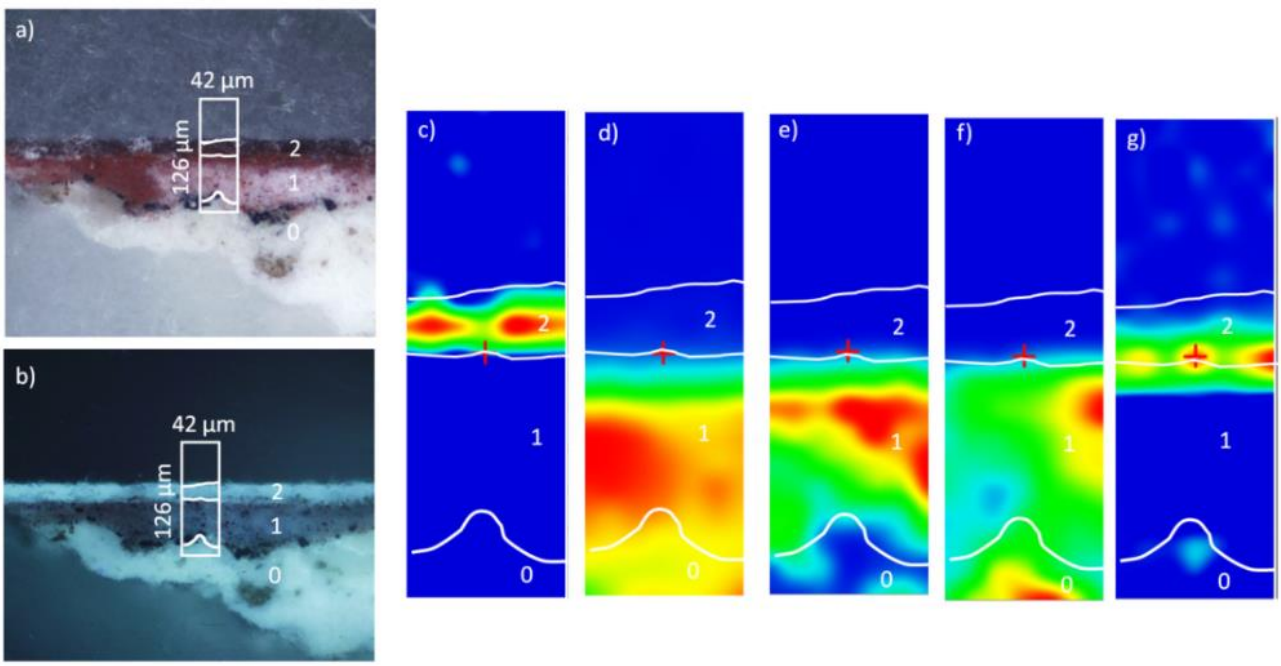

Fig. 2. Cross section photomicrographs of sample S1 a) visible light microscopic image; b) UV light microscopic image. The white box indicates the selected area for ATR-FTIR mapping analysis. FTIR false-colour plots representing c) Wax (peak area 730 cm^{-1}); d) Calcium carbonate (peak area 875 cm^{-1}); e) Silicates (peak area 1080 cm^{-1}); f) Calcium oxalates (peak area 1320 cm^{-1}); g) Calcium carboxylates.

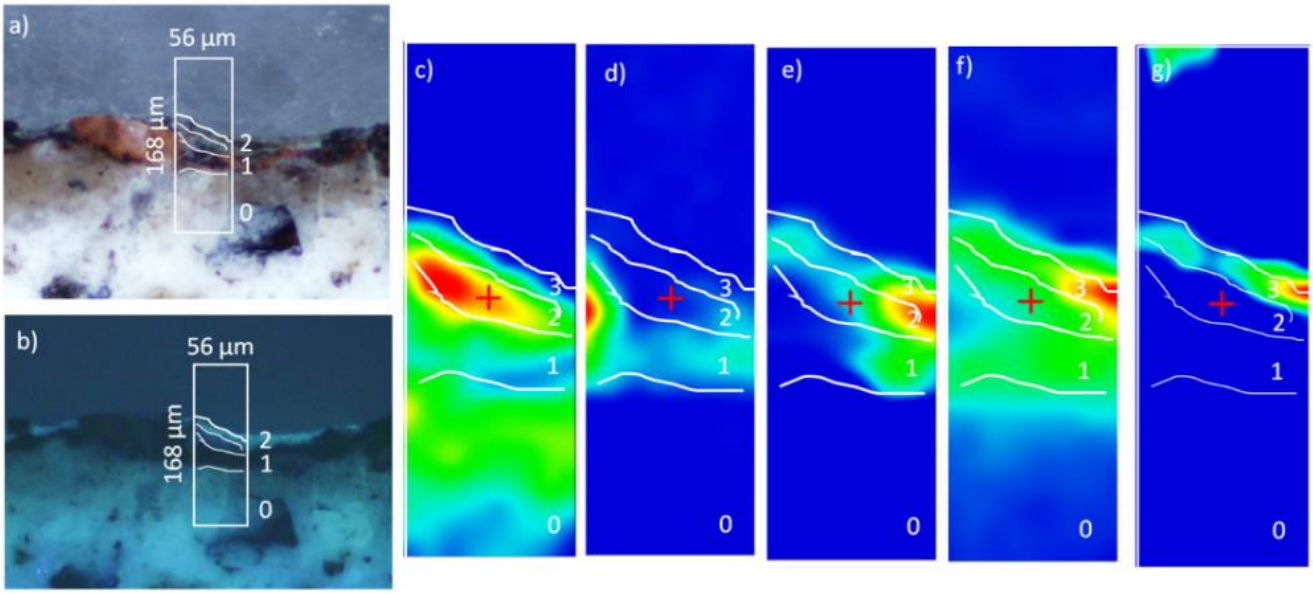

Fig. 3. Cross section photomicrographs of sample S2 a) visible light microscopic image; b) UV light microscopic image. The white box indicates the selected area for ATR-FTIR mapping analysis. FTIR false-colour plots representing c) Gypsum (peak area 3530 cm^{-1}); d) Silicates (peak area 790 cm^{-1}); e) Calcium oxalates (peak area 1320 cm^{-1}); f) Organic substances (peak area 2918 cm^{-1}); g) Fatty materials (peak area 1735 cm^{-1}).

In order to obtain more information about the chemical characterization of the translucent layer covering the wall painting surface, a sample S4 was collected from the bottom of the wall painting (region A1). The sample was investigated by ^{13}C CPMAS. Fig. 5 compares the ^{13}C CPMAS NMR spectrum of sample S4 (A) with the spectrum of a standard sample (B) obtained from an aged specimen made of beeswax on plaster. In the spectrum of the standard sample the strongest resonance centered between 30 and 35 ppm, is characteristic to the internal alkyl chain methylene (*int*-(CH_2)) carbons, and the resonance at about 15 ppm is due terminal methyl carbons of the chain. These

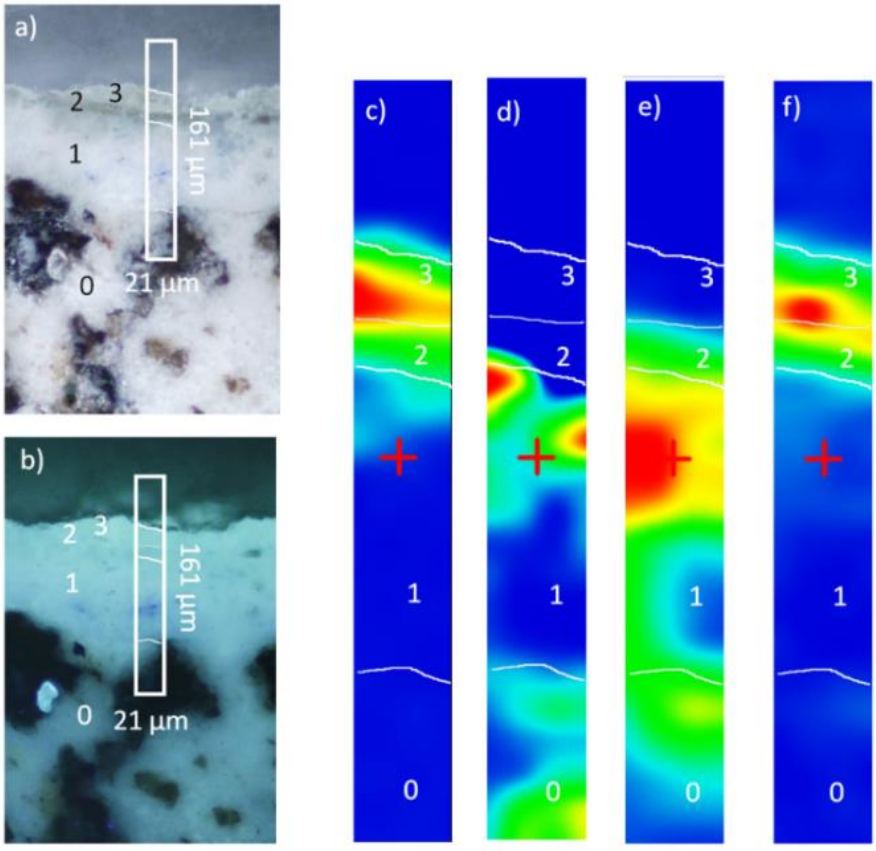

Fig. 4. Cross section photomicrographs of sample S3 a) visible light microscopic image; b) UV light microscopic image. The white box indicates the selected area for ATR-FTIR mapping analysis. FTIR false-colour plots representing c) Gypsum (peak area 3530 cm^{-1}); d) Silicates (peak area 990 cm^{-1}); e) Calcium carbonate (peak area 875 cm^{-1}); f) Organic substances (peak area 2918 cm^{-1}).

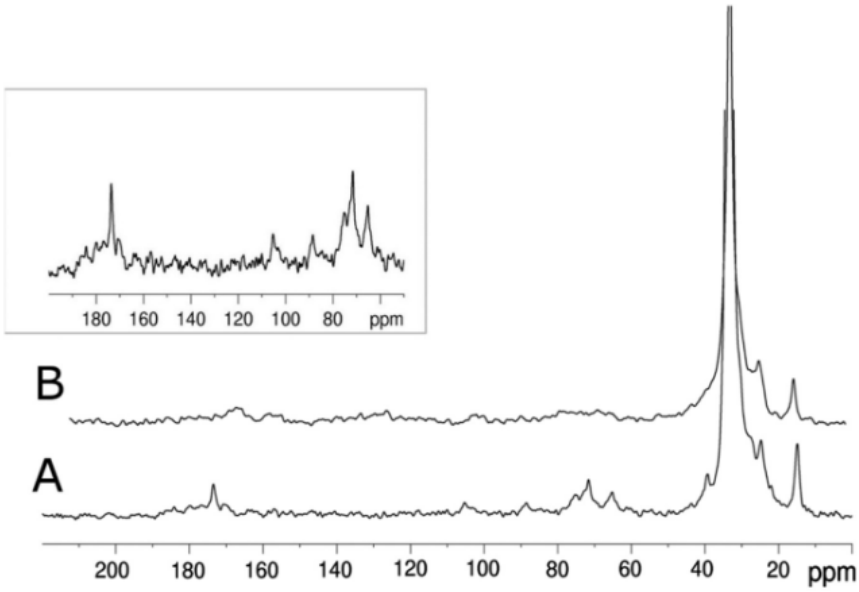

Fig. 5. ^{13}C CPMAS NMR spectrum of sample S4 (A) and the spectrum of a sample obtained from a specimen made of beeswax daubed on plaster (B). In the insert peaks resonating in the range of polysaccharides are shown with a vertical multiplication (4×).

resonances match those observed in the spectrum of S4 indicating that this sample is mainly constituted of beeswax. Furthermore, in this spectrum other weak resonances characteristic of polysaccharides are observed, see the insert in Fig. 5. Specifically, the resonance at 105 ppm is ascribable to C1 and the resonance at 89 ppm to C4, resonances between 70 and 75 ppm are due to C2, C3, and C5, and the resonance at 65 ppm is due to C6. The resonance at about 175 ppm arises from carboxylic groups (−COOH). These resonances might indicate the presence of starch or plant gum [30]. In the case of vegetable gum the signal at 175 ppm might arise from uronic acids [31].

In accordance with results obtained by IR mapping, ^{13}C CPMAS NMR spectroscopy confirmed that the translucent layer observed on some regions of the wall painting surface was constituted of beeswax. The presence of beeswax is likely to be due to previous restoration dated back to the 19th century.

To study in detail the complex stratigraphy of the wall painting made of alternating layers of organic and inorganic substances, a sample S5 was observed by optical and electron microscopy, see Fig. 6 (a–f). The analysis revealed the presence of a layer about 30 μm thick, constituted mainly by calcium, silicon and potassium (Fig. 6b, c, and d) which are elements belonging to the pictorial layer. Few single blue crystals included in the pictorial layer were also observable. Fig. 6e shows the EDS spectrum of a single blue crystal included in the pictorial layer which is likely to be due to lapis. The elemental composition of some white crystals belonging to the white internal layer was also analyzed by EDS possibly indicating the presence of sulphates, see Fig. 6e.

To fully characterize the molecular composition of salt efflorescences, three samples S6, S7, and S8 showing abundant efflorescences, were analyzed by XRD. In all samples, a notable amount of gypsum (G) was found, see Fig. 6g. A significant amount of calcite (C) belonging to the original material of the pictorial layer and plaster of the wall painting, was also detected in all samples, with S8 showing the highest amount. The highest amount of quartz (Q) was also detected in S8 whereas it was absent in S7.

The chemical characterization and the observation of the stratigraphy of the wall painting indicated a complex composition made of fatty materials and polysaccharides mixed with calcium carbonate, silicates, and pigments. These original materials alternate with degraded substances such as calcium oxalates, carboxylates and gypsum. It is worth to note that the highest concentration of calcium oxalates and carboxylates was observed close to layers rich in organic material. Oxalates are often found in cultural heritage objects, and their origin is still subject of debate in the scientific community [32–34]. The most prevalent hypothesis indicates a microbiological origin. According to Papliaka et al. the presence of calcium oxalates is presumably associated with the degradation of organic matter [35] and their position in the pictorial layer may allude to their origin being related to an organic binder or finishing layer. The presence of calcium carboxylates might be due to the interaction between metal ions present in pigments and fatty substances [36]. The presence of gypsum is probably due to rainwater percolation and infiltration from the roof that had caused the migration and crystallization of salts in the wall painting, and therefore the appearance of salt efflorescences on the wall painting surface. According to mapping analyses, the distribution of gypsum was high variable depending on the molecular composition of the stratigraphy of the wall painting. In those regions where organic material was present on the surface in a cohesive layer, the migration of salt efflorescences on the surface of the wall painting was impaired causing a significant gypsum accumulation at a deeper depth. In 2013 restoration works had been carried out in order to repair the roof and insulate the vault.

3.2. Evaluation of cleaning methods by portable non-invasive unilateral NMR and portable near FTIR spectroscopy

NMR stratigraphy encodes the amplitude of the ^{1}H NMR signal as a function of the depth scanned. Because different materials may contain different amounts of hydrogen, it is possible to ascribe layers containing different levels of hydrogen to different organic substances and to measure the thickness of the layers.

Unilateral NMR was applied to compare the performance of a microemulsion and a solvent gel cleaning treatment in removing the degraded beeswax layer. Fig. 7 shows ^{1}H NMR stratigraphies collected in areas M1 and M2 before and after cleaning treatments with microemulsion and solvent gel, respectively. In both cases, before the cleaning two portions of the profile with a different hydrogen content, namely R1 and R2 were encoded by the NMR stratigraphy. Before the cleaning in the first millimeter of depth, R1 showed an intense signal caused by the high hydrogen content of the beeswax layer. At a deeper depth, R2 showed a decrease of the signal due to the low hydrogen

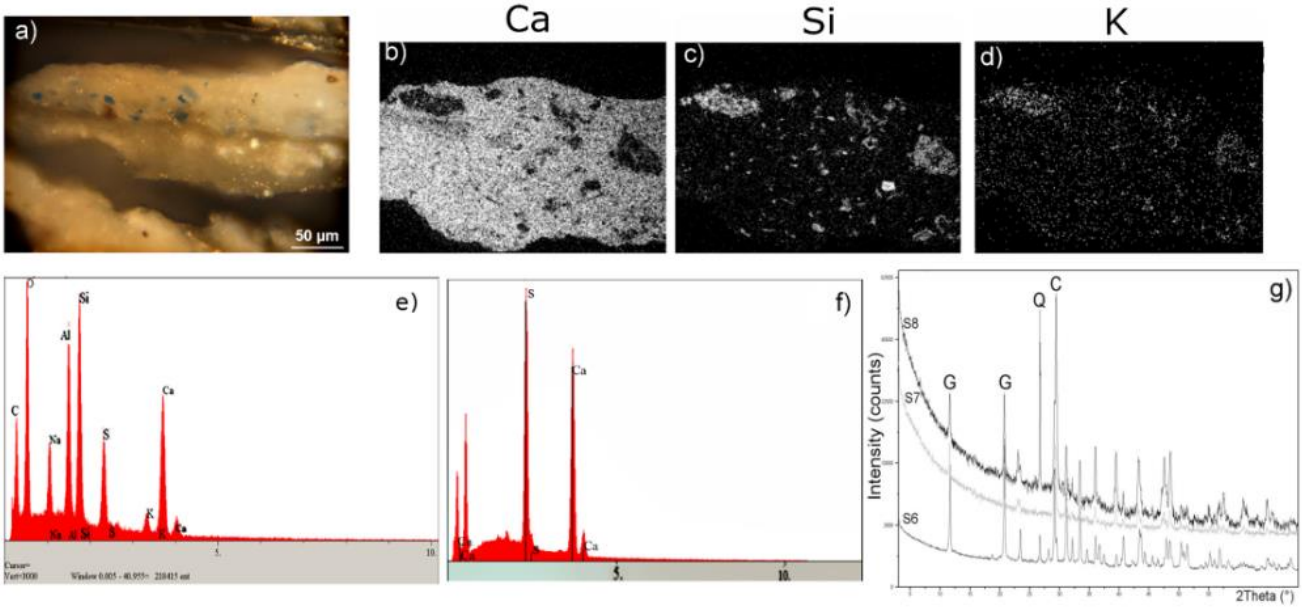

Fig. 6. a) OM image. b–d) Map of elements obtained by SEM-EDS of the cross-section of sample S5 collected from an area of the upper part of the wall painting (region A3) before the cleaning treatment. e) EDS spectrum of lapis. f) EDS spectrum of a white crystal. g) XRD spectra of samples S6, S7, and S8 collected from region A3 of the wall painting. G = gypsum, Q = quartz, C = calcite.

content of the plaster mainly constituted by inorganic materials. In both portions scanned (M1 and M2, see Fig. 1) the thickness of the beeswax layer was found to be about 400 μm. After the treatment with the solvent gel the NMR signal showed a slight decrease in region R1 and a thickness reduction to 200 μm, see Fig. 7a. After the cleaning treatment with the microemulsion the ^{1}H NMR stratigraphy showed a net decrease of the NMR signal in region R1 see Fig. 7b. As expected, after treatments no change of the signal intensity was observed in region R2 corresponding to the plaster.

The degree of solubilization of the cleaning treatment was calculated by the following equation:

$$R(\%) = \frac{I_{ut} - I_{tr}}{I_{ut} - I_0} * 100$$

where I_0 is the integral of the NMR stratigraphy of portion R2 calculated in the 2000–2500 μm range, and I_{ut} and I_{tr} are the integrals of

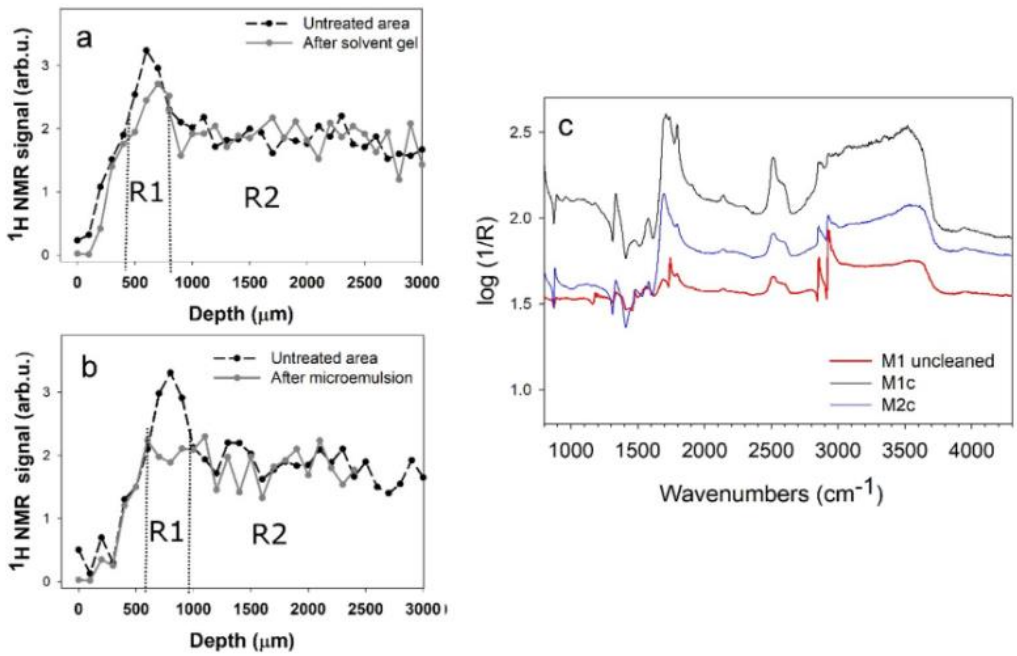

Fig. 7. a) ^{1}H NMR depth profiles of the uncleaned area M1 covered by the beeswax layer (black line) and the same region after the cleaning treatment with the solvent gel (gray line). b) ^{1}H NMR depth profiles of the uncleaned area M2 covered by the beeswax layer (black line) and the same region after the cleaning treatment with micro-emulsion (gray line). c) Near FTIR spectra collected in situ on the uncleaned area M1 showing a thick translucent layer, and spectra collected after cleaning treatments by microemulsion (M1c) and solvent gel (M2c), respectively.

portion R1 calculated in the 500–1000 μm range before and after the cleaning treatment, respectively. In the case of the micro-emulsion the degree of solubilization was found to be 92% whereas in the case of the solvent gel it was found to be 17%. These results provided evidence that the micro-emulsion removed much more material than solvent gel, nevertheless about 8% of beeswax was left after the cleaning with the micro-emulsion.

Results obtained by unilateral NMR were compared with those obtained by portable FTIR spectroscopy, see Fig. 7c. The spectrum of the uncleaned area (M1) showed the characteristic bands of beeswax. The reduction of the bands ascribed to beeswax was much more marked after the cleaning with the micro-emulsion (M1c) than the cleaning with the solvent gel (M2c). This observation confirmed the quantitative result obtained by unilateral NMR.

To study the properties of two hydrogel/bacteria cleaning systems and to evaluate the water distribution at the surface of the wall painting, unilateral NMR measurements were carried out. In the first step of work, water transport in Carbogel, and Vanzan gel was investigated by measuring the longitudinal relaxation time (T_1), the effective transverse relaxation time (T_{2eff}) and the self-diffusion coefficient D. As well known, relaxation times (T_1, T_2) of polymer-based hydrogels depend on the molecular weight of the polymer, degree of branching, crosslink density, size of the side groups, and temperature [37]. Furthermore, relaxation times depend on both rotational and translational molecular motions, whereas diffusion measurements are related only to the translational molecular displacement. T_1 and T_2 values found in Carbogel/bacteria, and Vanzan gels/bacteria cleaning systems are reported in Table 1. As reported in the literature [38], the transverse relaxation time (T_2) of a nucleus is sensitive to both slow and fast motions, while the longitudinal relaxation time (T_1) is affected by fast motions. The transverse relaxation time T_{2eff} was found to be much shorter than T_1 indicating that in both systems the water motion was slowed down by the presence of the polymeric network. The distributions of transverse relaxation times are reported in Fig. 8a. In the case of Carbogel two components of the transverse relaxation time T_{2a} and T_{2b} were found, the shortest one of 3.61 ms accounting for 8% and the longest one of 53.4 ms accounting for 92% of the total weight, respectively. Instead in Vanzan three components T_{2a}, T_{2b}, and T_{2c} of the transverse relaxation time were found, the shortest one of 3.2 ms, the intermediate one of 8.8 ms and the longest one of 53.5 ms accounting for 4%, 2%, and 94% of the total weight. It is well known that different states of water in hydrogels are characterized by different correlation times, which, in the absence of fast exchange, cause the onset of different transverse relaxation times [39]. In Carbogel/bacteria system the two T_2 components may be explained with the presence of two types of water. The shortest component may be ascribed to water in the first shell of solvation of the polymeric network involved in hydrogen bond and/or exchange with the network. The longest one may be ascribed to water free to move across the network. In the case of Vanzan a third component intermediate between the shortest and the longest ones is observed. This component is likely to be ascribed to water in a second shell of solvation, this water, even if not directly involved in hydrogen bonds with the polymeric network is affected by the presence of the network itself, and it is possibly in a slow exchange with water of the first solvation shell. The presence of different solvation shells in polymeric networks has been previously reported in literature [40,41].

To study the translational motion of water molecules in gel/bacteria systems, the self-diffusion coefficient was measured. Using unilateral NMR, the attenuation of the spin echo amplitude generated under a strong, uniform and static magnetic field gradient allows the measurement of the self-diffusion coefficient which gives information on molecular dynamics and sample microstructure [42,43]. Values of self-diffusion coefficients measured in Carbogel and Vanzan gel/bacteria systems are reported in Table 1. These values were found to be smaller than the self-diffusion coefficient of bulk water ($2.1 * 10^{-9}$ m^2/s at room temperature) indicating that the translational motion of water molecules was slightly hindered by the presence of the macromolecules.

The beeswax hydrophobicity strongly affects the wettability of the wall painting, as a consequence the capability of the cleaning system to release water may be affected by the presence of beeswax. ^{1}H NMR depth profiles were collected on the wall painting after the application of hydrogel/bacteria cleaning systems. Profiles collected before and after the beeswax removal are reported in Fig. 8b. After beeswax removal, the depth profile of the wall painting showed a remarkable increase of the absorbed water, a quantitative evaluation was carried out by numerical integration of the profile. Because in the ^{1}H NMR depth profile each point represents the amount of water at that depth, the integral of the depth profile is correlated to the total amount of water absorbed by the porous medium. In order to obtain the percentage of water saturation *WS* of the wall painting before and after the application of the cleaning treatment the following equation was applied:

$$WS = \frac{I_i - I_{min}}{I_{max} - I_{min}} * 100$$

where I_{min} is the integral of the profile obtained before the application of hydrogels/bacteria cleaning system, I_{max} is the integral of the profile at the longest time of application, and I_i is the integral of the profile at *i*th time of application. According to this equation in the case of the uncleaned area the *WS* value was found to be 62% with respect to the value calculated in the case of the cleaned area (100%), indicating that the removal of beeswax increased the wettability of about 40%.

^{1}H NMR depth profiles were also collected to evaluate the amount of water released by the gel/bacteria systems in the porous structure of the wall painting after 2- and 4-hours application, see Fig. 8c. The amplitude of depth profiles measured after 2-hours (*WS* 83%) and 4-hours application (*WS* 100%) of Carbogel/bacteria system were similar to each other indicating that the water releasing process from the cleaning system into the porous structure of the wall painting was almost complete after 2 h. Instead the amplitude of depth profiles measured after 4-hours application (*WS* 60%) of Vanzangel/bacteria system was found to be definitely higher than that collected after 2-hours application (*WS* 25%).

These results indicated that the kinetics of water absorption from the cleaning system to the porous structure depended on the type of gel as well as the time of application. Furthermore, according to results obtained by unilateral NMR, the wall painting displayed a better degree of wettability using Carbogel than Vanzan gel, proving Carbogel to be the best supporting material to subsume the bacteria suspension and convey bacteria through the porous structure.

The removal of salt efflorescences was evaluated by portable near FTIR spectra collected in situ before and after 2-hours application of Carbogel/bacteria and Vanzan gel/bacteria systems, see Fig. 8d and e.

Table 1
Relaxation times, relative weights of components, and self-diffusion coefficient measured in Carbogel/bacteria and Vanzan gel/bacteria cleaning systems.

	T_1 (s)	T_{2a} (ms)	W_a%	T_{2b} (ms)	W_b%	T_{2c} (ms)	W_c%	$D * 10^{-9}$ m^2/s
Carbogel 2%	1.7 ± 0.1	3.6	8	–	–	53.4	92	2.05 ± 0.01 (R^2 0.998)
Vanzan gel 3%	1.6 ± 0.1	3.2	4	8.8	2	53.5	94	1.99 ± 0.01 (R^2 0.998)

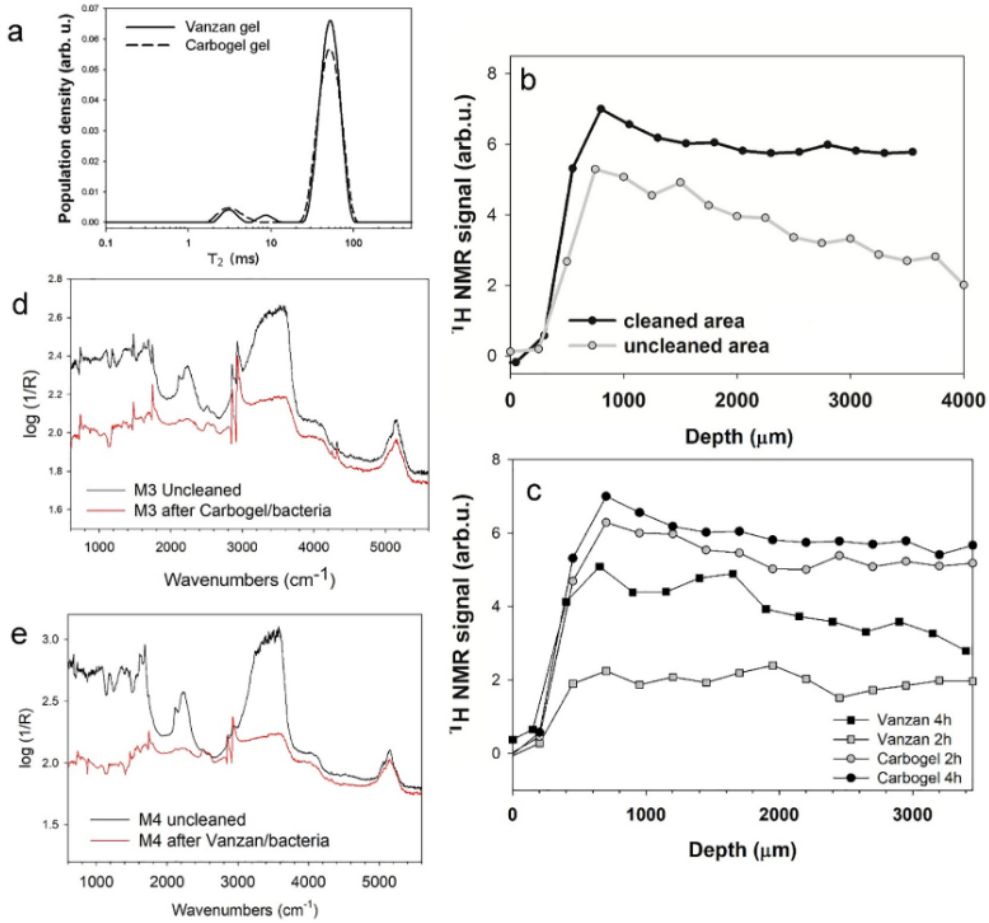

Fig. 8. a) Transverse relaxation time distributions of Vanzan gel/bacteria (solid line) and Carbogel/bacteria (dashed line) systems. b) ^{1}H NMR depth profiles of water absorbed in an uncleaned area of the wall painting (gray line) and a cleaned area where the beeswax layer had been previously removed (black line). c) ^{1}H NMR depth profiles of water released into the porous structure of the wall painting after applying the Carbogel/bacteria system for 2 (gray circles) and 4 h (black circles), and the Vanzan gel/bacteria system for 2 (gray squares) and 4 h (black squares).
Near FTIR spectra collected on areas M3 and M4 before and after 2-hours treatment with d) Carbogel/bacteria system and e) Vanzan gel/bacteria system respectively.

In both cases, after the cleaning treatment the bands at 2240 and 2350 cm^{-1} due to gypsum were reduced indicating the effectiveness of treatments to remove salt efflorescences.

Our results indicated that the presence of beeswax affected the performance of water-based cleaning systems inhibiting their action.

4. Conclusion

The achievement of the aim of our analytical study allowed to outline an analytical protocol using unilateral NMR to monitor and evaluate cleaning treatments directly in situ.

The analytical protocol was rationalized in terms of parameters obtained by a suitable process of the NMR data, namely *the solubilization degree of the cleaning system* and *the percentage of water saturation*. Unilateral NMR allowed to answer some questions such as the thickness of the beeswax layer to be removed, its distribution in the wall painting, and the presence of residues on the wall painting surface after the cleaning treatment. A suitable process of NMR data allowed the obtainment of the solubilization degree of cleaning systems permitting the selection of the most performing system. Furthermore, unilateral NMR was applied to evaluate changes in the permeability of the wall painting caused by the presence of organic substances during the application of water-based cleaning systems. The process of NMR data allowed to obtain the percentage of absorbed water before and after the application of the cleaning treatment. Furthermore, measurements performed by unilateral NMR allowed the obtainment of a detailed information about the interaction between water molecules, the gel network and the porous matrix. In order to assess which layers of the artefact were in contact with water during the application of the cleaning system, ^{1}H NMR depth profiles of water absorbed by the wall painting were collected. Depth profiles permitted the evaluation of the water content and its depth of penetration in the porous network. Relaxation times (T_1, T_2) and self-diffusion coefficients were measured to study the water molecular motions inside the gels in the presence of bacteria.

Our study demonstrated that in the case of wall paintings constituted by superficial organic layers, unilateral NMR was a very useful tool to analyze the thickness of these layers and to monitor the effect of the cleaning. In such cases, unilateral NMR allows a quantitative evaluation of residues of organic substances not removed by the cleaning, giving an evaluation of the cleaning power of the treatment. In addition, the penetration depth and the distribution of solvents used in cleaning treatments were obtained and monitored during the cleaning treatments and varying the time length.

Acknowledgment

The access to the MOLAB (CNR-ISTM) facility was supported by MIUR through the project IPERION CH.it in the frame of BIOREMP (biorestoration of mural painting). The present research was supported by Regione Lazio (Italy) within the ITER project "Infrastrutture, metodologie chimiche, nuove tecnologie applicate allo sviluppo delle imprese", bando Lr 13/2008. The authors thank Dr. Luisa Caporossi of the "Soprintendenza per l'Archeologia Belle Arti e Paesaggio per l'area metropolitana di Roma, la provincia di Viterbo e l'Etruria Meridionale, MIBACT, Rome, Italy and Giovanni Insolera, Curia of Civitavecchia-Tarquinia Civitavecchia, Rome, Italy, for promoting the restoration project of the chapel.

References

[1] R. Wolbers, Cleaning Painted Surfaces: Acqueos Methods, Archetype Publications, London, 2000.
[2] M. Koller, Surface cleaning and conservation, Conservation 15:3, The Getty Conservation Institute, Los Angeles, 2000, pp. 5–9.
[3] P. Baglioni, N. Bonelli, D. Chelazzi, A. Chavelier, L. Dei, J. Domengues, E. Fratini, R. Giorgi, M. Martin, Organogel formulations for the cleaning of easel paintings, Appl. Phys. A Mater. Sci. Process. 121 (2015) 857–868.
[4] G. Gautier, M.P. Colombini, GC–MS identification of proteins in wall painting samples: a fast clean-up procedure to remove copper-based pigment interferences, Talanta 73 (2007) 95–102.
[5] K. Kahrim, A. Daveri, P. Rocchi, G. de Cesare, L. Cartechini, C. Miliani, B.G. Brunetti, A. Sgamellotti, The application of in situ mid-FTIR fibre-optic reflectance spectroscopy and GC-MS analysis to monitor and evaluate painting cleaning, Spectrochim. Acta A 74 (2009) 1182–1188.
[6] N.N. Brandt, A.Yu. Chikishev, K. Itoh, N.L. Rebrikova, ATR-FTIR and FT Raman spectroscopy and laser cleaning of old paper samples with foxings, Laser Phys. 19 (2009) 483–492.
[7] E.A. Willneff, B.A. Ormsby, J.S. Stevens, C. Jaye, D.A. Fischer, S. Schroeder, Conservation of artists' acrylic emulsion paints: XPS, NEXAFS and ATR-FTIR studies of wet cleaning methods, Surf. Interface Anal. 46 (2014) 776–780.
[8] C. Canevali, M. Fasoli, M. Bertasa, A. Botteon, A. Colombo, V. Di Tullio, et al., A multi-analytical approach for the study of copper stain removal by agar gels, Micro. Chem. J 129 (2016) 249–258.
[9] F. Casanova, J. Perlo, B. Blümich, Single-Sided NMR, Springer Science & Business Media, 2011.
[10] J. Perlo, F. Casanova, B. Blümich, Profiles with microscopic resolution by single-sided NMR, J. Magn. Reson. 176 (2005) 64–70.
[11] M.D. Hürlimann, L. Venkataramanan, Quantitative measurement of two dimensional distribution functions of diffusion and relaxation in grossly inhomogeneous fields, J. Magn. Reson. 157 (2002) 31–42.
[12] B. Blümich, F. Casanova, J. Perlo, F. Presciutti, C. Anselmi, B. Doherty, Noninvasive testing of art and cultural heritage by mobile NMR, Acc. Chem. Res. 43 (2010) 761–770.
[13] E. Del Federico, S.A. Centeno, C. Kehlet, P. Currier, D. Stockman, A. Jerschow, Unilateral NMR applied to the conservation of works of art, Anal. Bioanal. Chem. 396 (2010) 213–220.
[14] D. Capitani, V. Di Tullio, N. Proietti, Nuclear magnetic resonance to characterize and monitor cultural heritage, Prog. Nucl. Magn. Reson. 64 (2012) 29–69.
[15] V. Di Tullio, D. Capitani, N. Proietti, Unilateral NMR to study water diffusion and absorption in stone-hydrogel systems, Microporous Mesoporous Mater. (2017), http://dx.doi.org/10.1016/j.micromeso.2017.07.011.
[16] V. Di Tullio, M. Cocca, R. Avolio, G. Gentile, N. Proietti, P. Ragni, M.E. Errico, D. Capitani, M. Avella, Magn. Reson. Chem. 53 (2014) 64–77.
[17] C. Kehlet, S. Nunberg, S. Alcala, J. Dittmer, Nuclear magnetic resonance analysis for treatment decisions: the case of a white sculptural environment by Louise Nevelson, Microchem. J. 137 (2018) 480–484.
[18] L.V. Angelova, B. Ormsby, E. Richardson, Diffusion of water from a range of conservation treatment gels into paint films studied by unilateral NMR: part I: acrylic emulsion paint, Microchem. J. 124 (2016) 311–320.
[19] C. Canevali, M. Fasoli, M. Bertasa, A. Botteon, A. Colombo, V. Di Tullio, et al., A multi-analytical approach for the study of copper stain removal by agar gels, Micro. Chem. J 129 (2016) 249–258.
[20] E. Del Federico, S.A. Centeno, C. Kehlet, K. Ulrich, A. Yamazaki-Kleps, A. Jerschow, In situ unilateral ^{1}H-NMR studies of the interaction between lead white pigments and collagen-based binders, Appl. Magn. Reson. 42 (2012) 363–376.
[21] E. Badea, C. Şendrea, C. Carşote, A. Adams, B. Bluemich, Unilateral NMR and thermal microscopy studies of vegetable tanned leather exposed to dehydrothermal treatment and light irradiation, Microchem. J. 129 (2016) 158–165.
[22] A. Venturi, Storia dell'Arte Italiana, VII, II, Milano, (1913), pp. 708–718.
[23] P. Baglioni, D. Berti, M. Bonini, E. Carretti, L. Dei, E. Fratini, R. Giorgi, Micelle, microemulsions, and gels for the conservation of cultural heritage, Adv. Colloid Interf. Sci. 205 (2014) 361–371.
[24] P. Baglioni, D. Chelazzi, Nanoscience for the Conservation of Works of Art, Royal Society of Chemistry, 2013.
[25] E. Gioventù, P.F. Lorenzi, F. Villa, C. Sorlini, M. Rizzi, A. Cagnini, A. Griffo, F. Cappitelli, Comparing the bioremoval of black crusts on colored artistic lithotypes of the Cathedral of Florence with chemical and laser treatment, Int. Biodeterior. Biodegrad. 65 (2011) 832–839.
[26] F. Troiano, D. Gulotta, A. Balloi, A. Polo, L. Toniolo, E. Lombardi, D. Daffonchio, C. Sorlin, F. Cappitelli, Successful combination of chemical and biological treatments for the cleaning of stone artworks, Int. Biodeterior. Biodegrad. 85 (2013) 294–304.
[27] G. Goelman, M.G. Prammer, The CPMG pulse sequence in strong magnetic field gradients with applications to oil-well logging, J. Magn. Reson. 113 (1995) 11–18.
[28] M.D. Hurlimann, D.D. Griffin, Spin dynamics of Carr-Purcell-Meiboom-Gill-like sequences in grossly inho-mogeneous B(0) and B(1) fields and application to NMR well logging, J. Magn. Reson. 143 (2000) 120–125.
[29] S. Prati, G. Sciutto, E. Catelli, A. Ashashina, R. Mazzeo, Development of innovative embedding procedures for the analyses of paint cross sections in ATR FTIR microscopy, Anal. Bioanal. Chem. 40 (2013) 895–905.
[30] O. Adeyanju, L. Lajide, O.O. Ajayi, I.A. Amoo, J. Plavec, Physicochemical and structural characterization of Sweitenia mycrophylla gum, Sch. Acad. J. Biosci. 3 (2015) 231–238.
[31] R.M.A. Daoub, A.H. Elmubarak, M. Misran, E.A. Hassan, M.E. Osman, Characterization and functional properties of some natural Acacia gums, J. Saudi Soc. Agric. Sci. (2016) 2016, http://dx.doi.org/10.1016/j.jssas.2016.05.002.
[32] M. Garcia-Vallès, M. Vendrell-Saz, J. Molera, F. Blázquez, Interaction of rock and atmosphere: patinas on Mediterranean monuments, Environ. Geol. 36 (1998) 137–149.
[33] F. Cariati, L. Rampazzi, L. Toniolo, A. Pozzi, Calcium oxalate films on stone surfaces: experimental assessment of the chemical formation, Stud. Conserv. 45 (2000) 180–188.
[34] P. Maravelaki-Kalaitzaki, Black crusts and patinas on Pentelic marble from the Parthenon and Erechtheum (Acropolis, Athens): characterization and origin, Anal. Chim. Acta 532 (2005) 187–198.
[35] Z.E. Papliaka, L. Vaccari, F. Zanini, S. Sotiropoulou, Improving FTIR imaging speciation of organic compound residues or their degradation products in wall painting samples, by introducing a new thin section preparation strategy based on cyclododecane pre-treatment, Anal. Bioanal. Chem. 407 (2015) 5393–5403.
[36] S. Sotiropoulou, Z. Papliaka, L. Vaccari, Micro FTIR imaging for the investigation of deteriorated organic binders in wall painting stratigraphies of different techniques and periods, Microchem. J. 124 (2016) 559–567.
[37] P.T. Challagan, Principles of Nuclear Magnetic Resonance Microscopy, Clarendon Press, Oxford, 1991.
[38] S.W. Homans, A Dictionary of Concepts in NMR, Clarendon Press, Oxford and New York, 1992.
[39] F. Müller-Plathe, Local structure and dynamics in solvent-swollen polymers, Macromolecules 31 (1998) 6721.
[40] D. Capitani, G. Mensitieri, F. Porro, N. Proietti, A.L. Segre, NMR and calorimetric investigation of water in a superabsorbing crosslinked network based on cellulose derivatives, Polymer 44 (2003) 6589–6598.
[41] D. Capitani, V. Crescenzi, A.A. De Angelis, A.L. Segre, Water in hydrogels. An NMR study of water/polymer interactions in weakly cross-linked chitosan networks, Macromolecules 34 (2003) 4136–4144.
[42] R. Kimmich, NMR: Tomography, Diffusiometry, Relaxometry, Springer, Berlin, 1997.
[43] D.G. Rata, F. Casanova, J. Perlo, D.E. Demco, B. Blümich, Self-diffusion measurements by a mobile single-sided NMR sensor with improved magnetic field gradient, J. Magn. Reson. 180 (2006) 229–235.